

UNIT-III

OPTICAL DETECTORS AND RECEIVERS

OPTICAL DETECTION PRINCIPLE:

The basic detection process in an intrinsic absorber is illustrated in Fig. 3.1 which shows a *pn* photodiode. This device is reverse biased and the electric field developed across the *pn* junction sweeps mobile carriers (holes and electrons) to their respective majority sides (*p* and *n* type material) a depletion region or layer is therefore created on either side of the junction. This barrier has the effect of stopping the majority carriers crossing the junction I. the opposite direction to the field. However, the field accelerates minority carriers from both sides to the opposite side of the junction, forming the reverse leakage current of the diode. Thus intrinsic conditions are created in the depletion region. A photon incident in or near the depletion region of this device which has an energy greater than or equal to the band gap energy Eg of the fabricating material (i.e. $hf \geq Eg$) will excite an electron from the valence band into the conduction band. This process leaves an empty hole in the valence band and is known as the photo generation of an electron hole (carrier) pair as shown in Fig. 3.1(a). Carrier pairs so generated near the junction are separated and swept (drift) under the influence of the electric field to produce a displacement current in the external circuit in excess of any reverse leakage current (Fig. 3.1(b)). Photo generation and the separation of a carrier pair in the depletion region of this reverse biased $\sim n$ junction is illustrated in Fig. 3.1(c).

Fig. 3.1 Operation of the *pn* photodiode: (a) photo generation of an electron hole pair in an intrinsic semiconductor.; (b) the structure of the reverse biased *pn* junction illustrating carrier drift in the depletion region: (c) the energy band diagram of the reverse biased *pn* junction showing photo generation and the subsequent separation of an electron hole pair. The depletion region must be sufficiently thick to allow a large fraction of the incident light to be absorbed in order to achieve maximum carrier pair generation. However, since long carrier drift times in the depletion region restrict the speed of operation of the photodiode it is necessary to limit its width. Thus there is a tradeoff between the number of photons absorbed (sensitivity) and the speed of response.

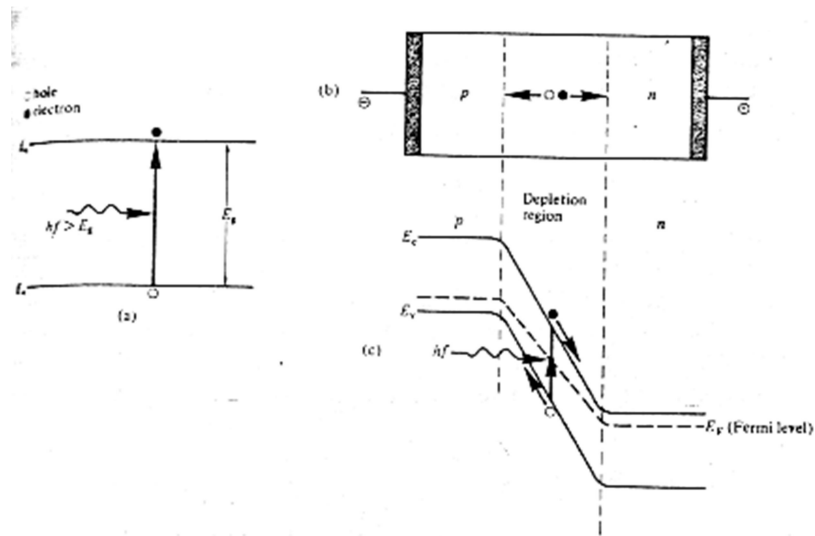


Fig. 3.1 Operation of the pn photodiode: (a) photo generation of an electron hole pair in an intrinsic semiconductor.; (b) The structure of the reverse biased pn junction illustrating carrier drift in the depletion region: (c) the energy band diagram of the reverse biased pn junction showing photo generation and the subsequent separation of an electron hole pair.

The depletion region must be sufficiently thick to allow a large fraction of the incident light to be absorbed in order to achieve maximum carrier pair generation. However, since long carrier drift times in the depletion region restrict the speed of operation of the photodiode it is necessary to limit its width. Thus there is a tradeoff between the number of photons absorbed (sensitivity) and the speed of response.

ABSORPTION:

Absorption Coefficient:

The absorption of photons in a photodiode to produce carrier pairs and thus a photocurrent, is dependent on the absorption coefficient α of the light in the semiconductor used to fabricate the device. At a specific wavelength and assuming only band gap transitions (i.e. intrinsic absorber) the photocurrent I_P produced by incident light of optical power P_0 is given by:

$$I_p = \frac{q}{h\nu} P_0 (1 - e^{-\alpha_s(\lambda)w}) (1 - R_f) \quad (3.1)$$

Where e is the charge on an electron, r is the Fresnel reflection coefficient at the semiconductor air interface and d is the width of the absorption region. The absorption coefficients of semiconductor materials are strongly dependent on wavelength. This is illustrated for some common semiconductors in Fig. 3.2. It may be observed that there is a variation between the absorption curves for the materials shown and that they are each suitable for different wavelength applications. This results from their differing band gaps energies as shown in Table 3.1. However, it must be noted that the curves depicted in Fig. 3.2 also vary with temperature. Fig. 3.2 Optical absorption curves for some common semiconductor photodiode materials (silicon, germanium, gallium arsenide and indium gallium arsenide phosphide). Table 3.1 Band gaps for some semiconductor photodiode materials at 300 K.

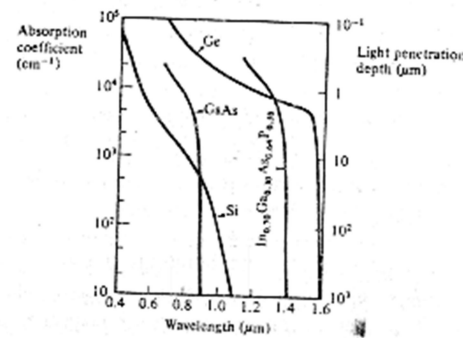


Fig. 3.2 Optical absorption curves for some common semiconductor photodiode materials (silicon, germanium, gallium arsenide and indium gallium arsenide phosphide).

Direct and Indirect Absorption: Silicon and Germanium Table 3.1 indicates that silicon and germanium absorb light by both direct and indirect optical transitions. Indirect absorption requires the assistance of a phonon so that momentum as well as energy is conserved. This makes the transition.

Table 8.1 Bandgaps for some semiconductor photodiode materials at 300 K

	Bandgap (eV) at 300 K	
	Indirect	Direct
Si	1.14	4.10
Ge	0.67	0.81
GaAs	—	1.43
InAs	—	0.35
InP	—	1.35
GaSb	—	0.73
In _{0.83} Ga _{0.17} As	—	0.75
In _{0.14} Ga _{0.86} As	—	1.15
GaAs _{0.88} Sb _{0.12}	—	1.15

Table 3.1 Band gaps for some semiconductor photodiode materials at 300 K

Probability less likely for indirect absorption than for direct absorption where no phonon is involved. In this context direct and indirect absorption may be contrasted with direct and indirect emission. Therefore as may be seen from Fig. 3.2 silicon is only weakly absorb over the wavelength band of interest in optical fiber communications (i.e. first generation 0.80.9 μ m). This is because transitions over this wavelength band in silicon are due only to the indirect absorption mechanism. As mentioned previously (Section 3.2) the threshold for indirect absorption occurs at 1.09 μ m. The band gap for direct absorption in silicon is 4.10 eV corresponding to a threshold of 0.30 μ m in the ultraviolet and thus is well outside the wavelength range of interest. Germanium is another semiconductor material for which the lowest energy absorption takes place by indirect optical transitions. However, the threshold for direct absorption occurs at 1.53 μ m, below which germanium becomes strongly absorbing corresponding to the kink in the characteristic shown in Fig. 3.2. Thus germanium may be used in the fabrication of detectors over the whole of the wavelength range of interest (i.e. first and second generation 0.81.3 μ m), especially considering that indirect absorption will occur up to a threshold of 1.85 μ m. Ideally a photodiode material should be chosen with band gap energy lightly less than the photon energy corresponding to the longest operating wavelength of the system. This gives a sufficiently high absorption coefficient ensure a good response, and yet limits the number of thermally generated carriers in order to achieve a low dark current (i.e.

displacement current generated with no incident light (see Fig. 3.5)). Germanium photodiodes have relatively large dark currents due to their narrow band gaps in comparison to other semiconductor materials. This is a major disadvantage with the use of germanium photodiodes especially at shorter wavelengths (below 1.1 um). 3.4.3 IIIV Alloys The drawback with germanium as a fabricating material for semiconductor photodiodes has led to increased investigation of direct band gap IIIV alloys for the

longer wavelength region. These materials are potentially superior to germanium because their band gaps can be tailored to the desired wavelength by changing the relative concentrations of their constituents, resulting in lower dark currents. They may also be fabricated in hetero junction structures which enhances their high speed operation. Ternary alloys such as InGaAs and GaAlSb deposited on GaSb substrate have been used to fabricate photodiodes for the $1.0 \sim 1.4 \text{ } \mu\text{m}$ wavelength. However, difficulties in growth of these alloys with lattice matching have led to defects which cause increased dark currents and micro plasma sites (such areas with lower breakdown voltages than the rest of the junction). These defects limit the performance of a device fabricated from ternary alloys. More encouraging results have been obtained with quaternary alloys such as InGaAsP grown on InP and GaAlAsSb grown on GaSb. These systems have the major advantage that the band gap and lattice constant can be varied independently. This permits the band gap tailoring whilst maintaining a lattice match to the substrate.

QUANTUM EFFICIENCY:

The quantum efficiency is defined as the fraction of incident photons which are absorbed by the photo detector and generate electrons which are collected at the detector terminals:

$$\eta = \frac{\text{number of electron-hole pairs generated}}{\text{number of incident-absorbed photons}} = \frac{I_p / q}{P_{in} / h\nu}$$

and

$$\eta = \frac{r_e}{r_p}$$

Where r_p is the incident photon rate (photons per second) and r_e is corresponding electron rate (electrons per second).

One of the major factors which determine the quantum efficiency is absorption coefficient (see Section 3.4.1) of the semiconductor material used within the photo detector. It is generally less than unity as not all of the incident photons are absorbed to create electron hole pairs. Furthermore, it should be noted that the quantum efficiency is often quoted as a percentage (e.g. a quantum efficiency of 75% is equivalent to 75 electrons collected per 100 incident photons). Finally, in common with the absorption coefficient, quantum efficiency is a function of the photon wavelength and must therefore only be quoted for a specific wavelength.

RESPONSIVITY:

The expression for quantum efficiency does not involve photon energy and therefore the responsivity R is often of more use when characterizing the performance of a photo detector. It is defined as:

$$R = I_p / P_0 \text{ A W}^{-1} \quad (3.4)$$

Where I_p is the output photocurrent in amperes and P_0 is the incident optical power in watts. The responsivity is a useful parameter as it gives the transfer characteristic of the detector (i.e. photocurrent per unit incident optical power).

The relationship for responsivity (Eq (3.4)) may be developed to include quantum efficiency as follows. Considering equation the energy of a photon $E = hf$ Thus the incident photon rate r_p may be written in terms of incident optical power and the

Photon energy as:

$$r_p = P_0 / hf \quad \text{----- (3.5)}$$

In Eq. (3.3) the electron rate is given by:

$$r_e = \eta r_p \quad (3.3)$$

Substituting from Eq. (3.5) we obtain

$$r_e = \eta P_o / hf \quad (3.7)$$

Therefore, the output photocurrent is:

$$I_p = \eta P_o e / hf \quad (3.8)$$

where e is the charge on an electron. Thus from Eq. (3.4) the responsivity may be

Written as:

$$R = \eta e / hf \quad (3.9)$$

Equation (3.9) is a useful relationship for responsivity which may be developed further stage to include the wavelength of the incident light.

The frequency f of the incident photons is related to their wavelength λ and the velocity of light in air C , by:

$$f = c / \lambda \quad (3.10)$$

Substituting into Eq. (3.9) a final expression for the responsivity is given by:

$$R = \eta e \lambda / hc \quad (3.11)$$

It may be noted that the responsivity is directly proportional to the quantum efficiency at a particular wavelength.

The ideal responsivity against wavelength characteristic for a silicon photodiode with unit quantum efficiency is illustrated in Fig. 3.3. Also shown is the typical responsivity of a practical silicon device.

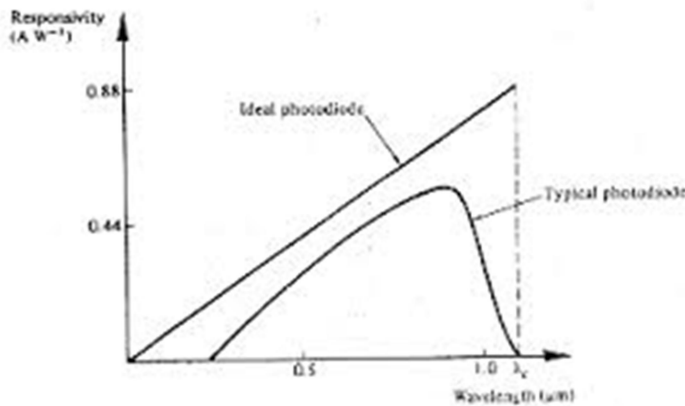


Fig. 3.3 Responsivity against wavelength characteristic for ideal silicon

Photodiode The responsivity of a typical device is also shown.

LONG WAVELENGTH CUTOFF

It is essential when considering the intrinsic absorption process that the energy of incident photons be greater than or equal to the band gap energy E_g of the material used to fabricate the photo detector. Therefore, the photon energy

$$h\nu / \lambda \geq E_g \quad (3.12)$$

Giving

$$\lambda \leq hc/E_g \quad (3.13)$$

Thus the threshold for detection, commonly known as the long wavelength cutoff

Point is:

$$\lambda_c = hc/E_g \quad (3.14)$$

The expression given in above allows the calculation of the longest wavelength of light to give photo detection for the various semiconductor materials used in the fabrication of detectors.

It is important to note that the above criterion is only applicable to intrinsic photo detectors. Extrinsic photo detectors violate the expression given in Eq. (3.12), but are not currently used in optical fiber communications.

SEMICONDUCTOR PHOTODIODES WITHOUT INTERNAL GAIN:

Semiconductor photodiodes without internal gain generate a single electron hole pair per absorbed photon. This mechanism was outlined in Section 3.3, and in order to understand the development of this type of photodiode it is now necessary to elaborate upon it.

pn photodiode:

Figure 3.4 shows a reverse biased *pn* photodiode with both the depletion and diffusion regions. The depiction region is formed by immobile positively charged donor atoms in the n type semiconductor material and immobile negatively charged acceptor atoms in the p type material, when the mobile carriers are swept to their majority sides under the influence of the electric field. The width of the depletion region is therefore dependent upon the doping concentrations for a given applied reverse bias (i.e. the lower the doping, the wider the depletion region).

Photons may be absorbed in both the depletion and diffusion regions, as indicated by the absorption region in Figure 3.4. The absorption region's position and width depends upon the energy of the incident photons and on the material from which the photodiode is fabricated. Thus in the case of the weak absorption of photons, the absorption region may extend completely throughout the device. Electron hole pairs are therefore generated in both the depletion and diffusion regions. In the depletion region the carrier pairs separate and drift under the influence of the electric field, whereas outside this region the hole diffuses towards the depletion region in order to be collected. The diffusion process is very slow compared to drift and thus limits the response of the photodiode (see Section 3.8.3).

It is therefore important that the photons are absorbed in the depletion region. Thus it is made as long as possible by decreasing the doping in the n type material. The depletion region width in a *pn* photodiode is normally 1 to 3 μm and is optimized for the efficient detection of light at a given wavelength. For silicon devices this is in the visible spectrum (0.4 to 0.7 μm) and

for germanium in the near infrared (0.7 to 0.9 μm). Typical output characteristics for the reverse biased photodiode are illustrated in Figure 3.5. The different operating conditions may be noted moving from no light input to a high light level.

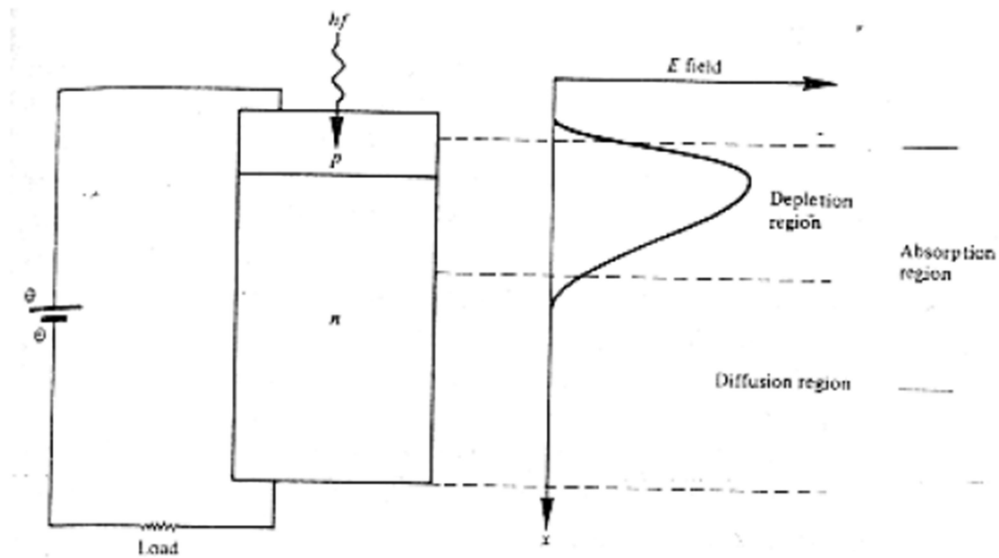


Figure 3.4 pn photodiode showing depletion and diffusion regions.

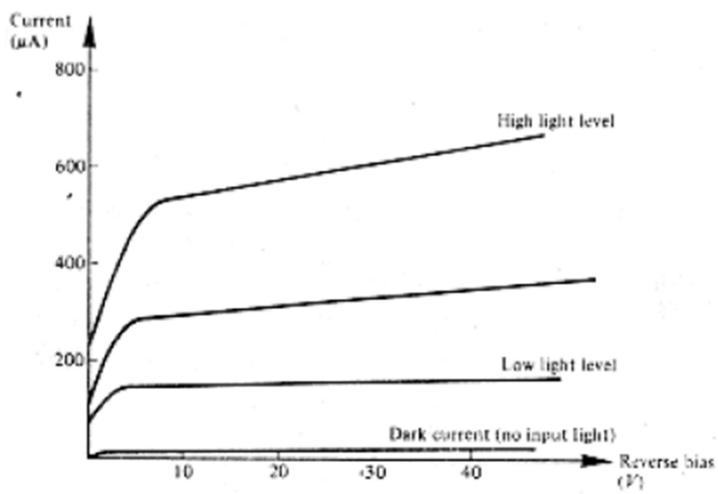


Figure 3.5 Typical pn photodiode output characteristic

pin photodiode:

In order to allow operation at longer wavelengths where the light penetrates more deeply into the semiconductor material a wider depletion region is necessary. To achieve this the n type material is doped so lightly that it can be considered intrinsic, and to make a low resistance contact a highly doped n type (n^+) layer is added. This creates a *pin* (or PIN) structure as may be seen in Figure 3.3 where all the absorption takes place in the depletion region.

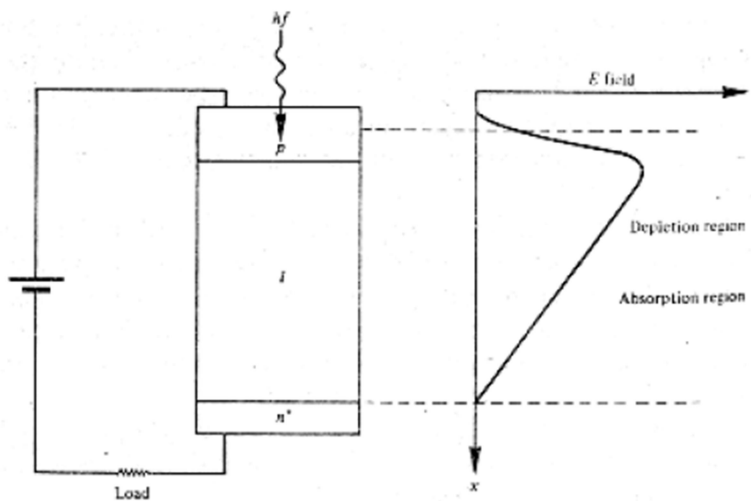


Figure 3.3 pin photodiode showing combined absorption and depletion region

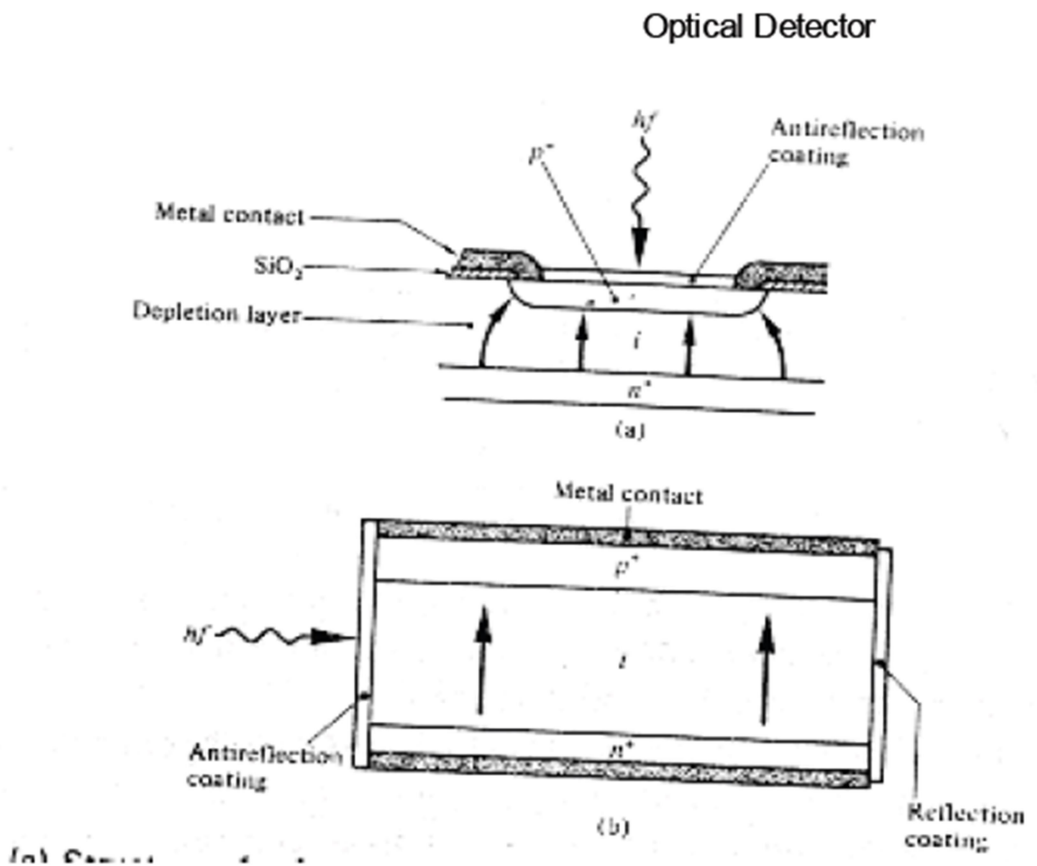


Figure 3.7 (a) Structure of a front illuminated silicon pin photodiode

Figure 3.7 shows the structures of two types of silicon pin photodiode for operation in the shorter wavelength band below $1.09\mu m$. The front illuminated photodiode, when operating in the 0.8 to 0.9 nm band (Figure 3.7(a)), requires a depletion region of between 20 and 50 μm in order to attain high quantum efficiency (typically 850%) together with fast response (less than 1 ns) and low dark current (1 nA). Dark current arises from surface leakage currents as well as generation-recombination currents in the depletion region in the absence of illumination. The side illuminated structure (Figure 3.7(b)), where light is injected parallel to the junction plane, exhibits a large absorption width ($= 500\mu m$) and hence is particularly sensitive at wavelengths close to the bandgap limit ($1.09\mu m$) where the absorption coefficient is relatively small.

Germanium pin photodiodes which span the entire wavelength range of interest are also commercially available, but as mentioned previously (Section 3.4.2) the relatively high dark

current are a problem (typically 100 nA at 20 °C increasing to 1 μA at 40°C). However, as outlined in Section 3.4.3, IIIV semiconductor alloys are under investigation for detection in the longer wavelength region. The two particular interest in view of lattice matching are $\text{In}_{1-x}\text{Ga}_x\text{As}_y\text{P}_{1-y}$ grown on InP and $\text{Ga}_x\text{Al}_{1-x}\text{As}_y\text{Sb}_{1-y}$ on GaSb. The structure for a pinphotodiode of the former is shown in Fig. 3.8.

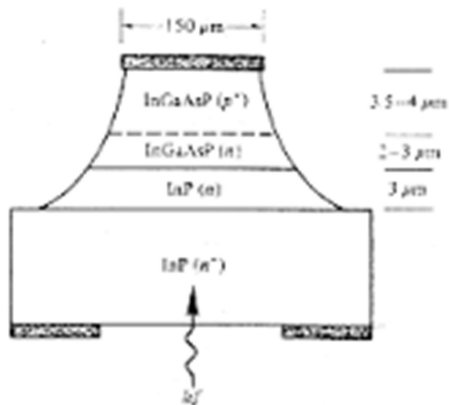


Figure 3.8 Structure of an InGaAsP pIn photodiode. The InP base is transparent to the radiation absorbed in the quaternary layers.

SEMICONDUCTOR PHOTODIODES WITH INTERNAL GAIN:

Avalanche photodiode:

The second major type of optical communications detector is the avalanchephotodiode (APD). This has a more sophisticated structure than the *pin*photodiode in order to create an extremely high electric field region (approximately 3×10^5 V cm⁻¹), as may be seen in Figure 3.9(a). Therefore, as well as the depletion region where most of the photons are absorbed and the primary carrier pairs generated there is a high field region in which holes and electrons can acquire sufficient energy to excite new electronhole pairs. This process is known as impactionization and is the phenomenon that leads to avalanche breakdown in ordinary reverse biased diodes. It often requires high reverse bias voltages (100 to 400 V) in order that the new carriers created by impact ionization can themselves produce additional carriers by the same mechanism as shown in Figure 3.9(b).

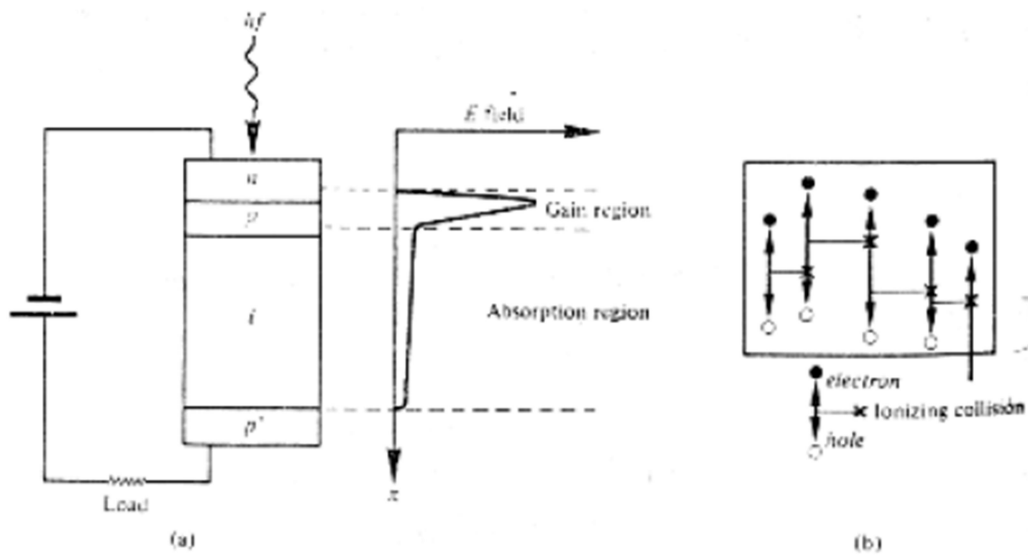


Figure 3.9 (a) Avalanche photodiode showing high electric field (gain) region

(b) Carriers pair multiplication in the gain region

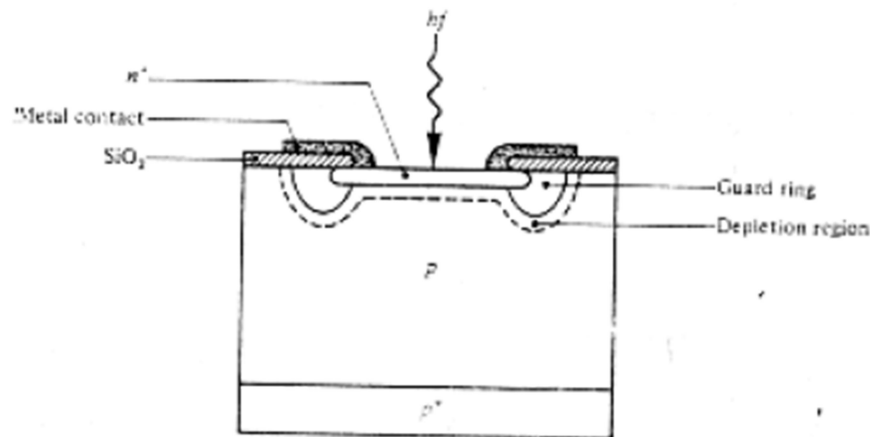


Figure 3.10 Structure of a silicon avalanche photodiode with guard ring

Carrier multiplication factors as great as 104 may be obtained using defectfree materials to ensure uniformity of carrier multiplication over the entire photosensitive area. However, other factors affect the achievement of high gain within the device. Microplasmas, which are small areas with lower breakdown voltages than the remainder of the junction, must be reduced

through the selection of defect free materials together with careful device processing and fabrication [Ref. 141]. In addition, excessive leakage at the junction edges can be eliminated by the use of a guard ring structure as shown in Figure 3.12. At present both silicon and germanium APDs are available.

Operation of these devices at high speed requires full depletion in the absorption region. As indicated in Section 3.8.1, when carriers are generated in undepleted material, they are collected somewhat slowly by the diffusion process. This has the effect of producing a long 'diffusion tail' on a short optical pulse. When the APD is fully depleted by employing electric fields in excess of 10^4 V m⁻¹, all the carriers drift at saturation limited velocities. In this case the response time for the device is limited by three factors. These are:

- (a) the transit time of the carriers across the absorption region (i.e. the depletion width);
- (b) the time taken by the carriers to perform the avalanche multiplication process; and
- (c) the RC time constant incurred by the junction capacitance of the diode and its load.

At low gain the transit time and RC effects dominate giving a definitive response time and hence constant bandwidth for the device. However, at high gain the avalanche buildup time dominates and therefore the device bandwidth decreases proportionately with increasing gain. Such APD operation is distinguished by a constant gain bandwidth product. Often an asymmetric pulse shape is obtained from the APD which results from a relatively fast rise time as the electrons are collected and a fall time dictated by the transit time of the holes travelling at a slower speed. Hence, although the use of suitable materials and structures may give rise times between 150 and 200 ps, fall times of 1 ns or more are quite common which limit the overall response of the device.

Silicon reach through avalanche photodiodes:

To ensure carrier multiplication without excess noise for a specific thickness of multiplication region within the APD it is necessary to reduce the ratio of the ionization coefficients for electrons and holes k (see Section 3.3.4). In silicon this ratio is a strong function of the electric field varying from around 0.1 at 3×10^5 V m⁻¹ to 0.5 at 3×10^5 V m⁻¹. Hence for minimum noise, the electric field at avalanche breakdown must be as low as possible and the

impact ionization should be initiated by electrons. To this end a 'reach through' structure has been implemented with the silicon avalanche photodiode. The silicon 'reach through' APD(RAPD) consists of p^{++} pie'pn⁺ layers as shown in Figure 3.13(a). As may be seen from the corresponding field plot in Figure 3.13(b), the high field region where the avalanche multiplication takes place is relatively narrow and centered on the pn⁺ junction. Thus under low reverse bias most of the voltage is dropped across the pn⁺ junction.

When the reverse bias voltage is increased the depletion layer widens across the p region until it 'reaches through' to the nearly intrinsic (lightly doped) 'pie' region. Since the 'pie' region is much wider than the p region the field in the 'pie' region is much lower than that at the pn⁺ junction (see Figure 3.13(b)). This has the effect of removing some of the excess applied voltage from the multiplication region to the 'pie' region giving a relatively slow increase in multiplication factor with applied voltage. Although the field in the 'pie' region is lower than in the multiplication region it is high enough (2×10^4 Vcm⁻¹) when the photodiode is operating to sweep the carriers through to the multiplication region at their scattering limited velocity (107 cm s⁻¹). This limits the transit time and ensures a fast response (as short as 0.5 ns).

Measurements for a silicon RAPD for optical fiber communication applications at a wavelength of 0.825 micro meter have shown a quantum efficiency (without avalanche gain) of nearly 100% in the working region, as may be seen in Figure 3.14. The dark currents for this photodiode are also low and depend only slightly on bias voltage.

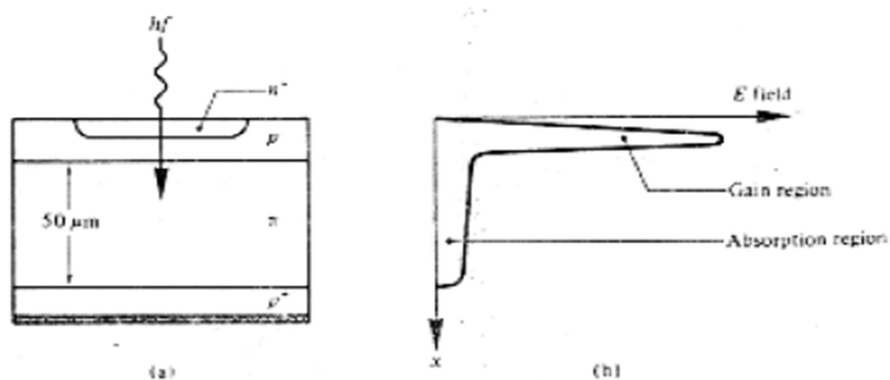


Figure 3.11 (a) Structure of a silicon RAPD(b) The field distribution in the RAPD showing the gain region across the pn⁺ junction.

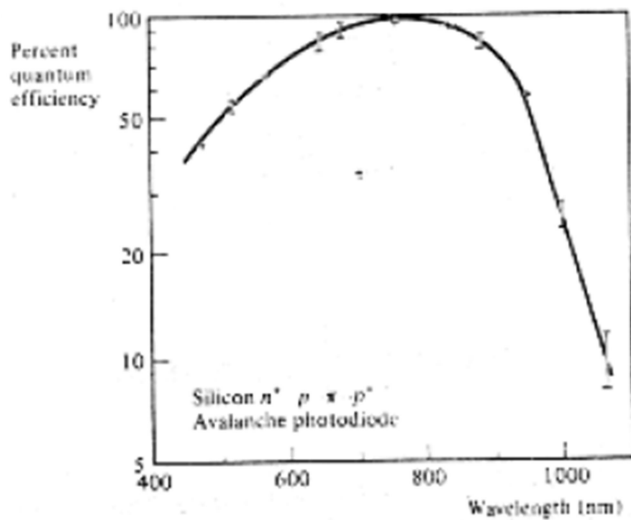


Figure 3.12 Measurement of quantum efficiency against wavelength for a silicon RAPD.

Benefits and drawbacks with the avalanche photodiode:

APDs have a distinct advantage over photodiodes without internal gain for the detection of the very low light levels often encountered in optical fiber communications. They generally provide an increase in sensitivity of between 5 and 15 dB over *pin* photodiodes whilst often giving a wider dynamic range as a result of their gain variation with response time and reverse bias. The optimum sensitivity improvement of APD receivers over *pin* photodiode devices is illustrated in the characteristics shown in Figure 3.21. The characteristics display the minimum detectable optical power for direct detection versus the transmitted bit rate in order to maintain a bit error rate (BER) or 10⁻⁹ (see Section 11.3.3) in the shorter and longer wavelength regions. Figure 3.21(a) compares silicon photodiodes operating at a wavelength of 0.82 mm where the APD is able to approach within 10 to 13 dB of the quantum limit. In addition, it may be observed that the *pin* photodiode receiver has a sensitivity around 15 dB below this level. InGaAs photodiodes operating at a wavelength of 1.55 are compared in Figure 3.21(b). In this case the APD requires around 20 dB more power than the quantum limit, whereas the *pin* photodiode receiver is some 10 to 12 dB less sensitive than the APD. APDs, however, also have several drawbacks which include:

- (a) fabrication difficulties due to their more complex structure and hence increased
- (b) the random nature of the gain mechanism which gives an additional noise contribution ;
- (c) the often high bias voltages required (50 to 400 V) which are wavelength dependent;
- (d) the variation of the gain (multiplication factor) with temperature as shown in Figure 3.22 for a silicon RAPD; thus temperature compensation is necessary to stabilize the operation of the device.

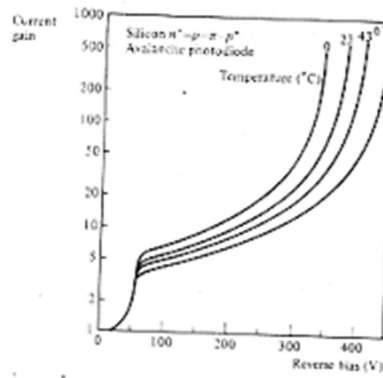


Figure 3.14 Current gains against reverse bias for a silicon RAPD operating at a wavelength of 0.825μm.

Multiplication factor:

The multiplication factor M is a measure of the internal gain provided by the APD. It is defined as:

$$M = \frac{I}{I_p}$$

where I is the total output current at the operating voltage (i.e. where carrier multiplication occurs) and I_p is the initial or primary photocurrent (i.e. before carrier multiplication occurs)

RECEIVER PERFORMANCE AND CALCULATIONS:

NOISE:

INTRODUCTION:

The receiver in an intensity modulated/direct detection (IM/DD) optical fiber communication system essentially consists of the photo detector plus an amplifier with possibly additional signal processing circuits. Therefore the receiver initially converts the optical signal incident on the detector into an electrical signal, which is then amplified before further processing to extract the information originally carried by the optical signal.

It is essential that the detector performs efficiently with the following amplifying and signal processing circuits. Inherent to this process is the separation of the information originally contained in the optical signal from the noise generated within the rest of the system and in the receiver itself, as well as any limitations on the detector response imposed by the associated circuits. These factors play a crucial role in determining the performance of the system.

In order to consider receiver design it is useful to regard the limit on the performance of the system set by the signal to noise ratio (SNR) at the receiver. It is therefore necessary to outline noise sources within optical fiber systems. The noise in these systems has different origins from that of copper based systems. Both types of system have thermal noise generated in the receiver. However, although optical fiber systems exhibit little crosstalk the noise generated within the detector must be considered, as well as the noise properties associated with the electromagnetic carrier.

In Section 3.10.2 we therefore briefly review the major noise mechanisms which are present in direct detection optical fiber communication receivers prior to more detailed discussion of the limitations imposed by photon (or quantum) noise in both digital and analog transmission. This is followed in Section 3.10.3 with a more specific discussion of the noise associated with the two major receiver types (i.e. employing *pin* and avalanche photodiode detectors). Expressions for the SNRs of these two receiver types are also developed in this section. Section 3.10.4 considers the noise and bandwidth performance of common preamplifier structures utilized in the design of optical fiber receivers. In Section 3.10.4.1 we present a brief

account of low noise field effect transistor (FET) preamplifiers which find wide use within optical fiber communication receivers. This discussion also includes consideration of *Pin* photodiode/FET (PINFET) hybrid receiver circuits which have been developed for optical fiber communications. Finally, major high performance receiver design strategies to provide low noise and high bandwidth operation as well as wide dynamic range are described in Section 3.10.4.2.

Noise is a term generally used to refer to any spurious or undesired disturbances that mask the received signal in a communication system. In optical fiber communication systems we are generally concerned with noise due to spontaneous fluctuations rather than erratic disturbances which may be a feature of copper based systems (due to electromagnetic interference, etc.).

There are three main types of noise due to spontaneous fluctuations in optical fiber communication systems: thermal noise, dark current noise and quantum noise.

Thermal noise:

This is the spontaneous fluctuation due to thermal interaction between, say, the free electrons and the vibrating ions in a conducting medium, and it is especially prevalent in resistors at room temperature. The thermal noise current i , in a resistor R may be expressed by its mean square value [Ref. 1] and is given by:

$$\overline{i_t^2} = \frac{4KTB}{R}$$

where K is Boltzmann's constant, T is the absolute temperature and B is the post detection (electrical) bandwidth of the system (assuming the resistor is in the optical receiver).

where K is Boltzmann's constant, T is the absolute temperature and B is the post detection(electrical) bandwidth of the system (assuming the resistor is in the optical receiver).

$$\overline{i_d^2} = 2eBI_d$$

where e is the charge on an electron and I_d is the dark current. It may be reduced by careful design and fabrication of the detector.

Quantum noise:

The quantum nature of light was discussed in Section 3.2.1 and the equation for the energy of this quantum or photon was stated as $E = hf$. The quantum behavior of electromagnetic radiation must be taken into account at optical frequencies since $hf > KT$ and quantum fluctuations dominate over thermal fluctuations. The detection of light by a photodiode is a discrete process since the creation of an electronhole pair results from the absorption of a photon, and the signal emerging from the detector is dictated by the statistics of photon arrivals. Hence the statistics for monochromatic coherent radiation arriving at a detector follows a discrete probability distribution which is independent of the number of photons previously detected. It is found that the probability $P(z)$ of detecting z photons in time period τ when it is expected on average to detect z . photons obeys the Poisson distribution :

$$P(z) = \frac{z^z \exp(-z_m)}{z!}$$

where z_m is equal to the variance of the probability distribution. This equality of the mean and the variance is typical of the Poisson distribution. From Eq. (3.7) the electron rate r_c , generated by incident photons is $r_e = P_o / hf$. The number of electrons generated in time is equal to the average number of photons detected over this time period z . Therefore:

$$z_m = \frac{\eta P_o \tau}{hf}$$

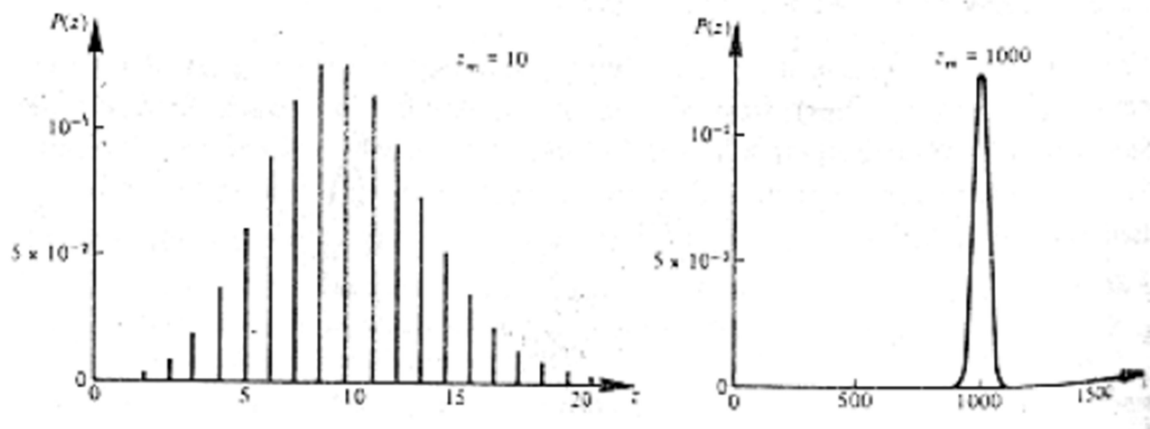


Figure 3.10.1 Poisson distributions for $z_m = 10$ and $z_m = 1000$.

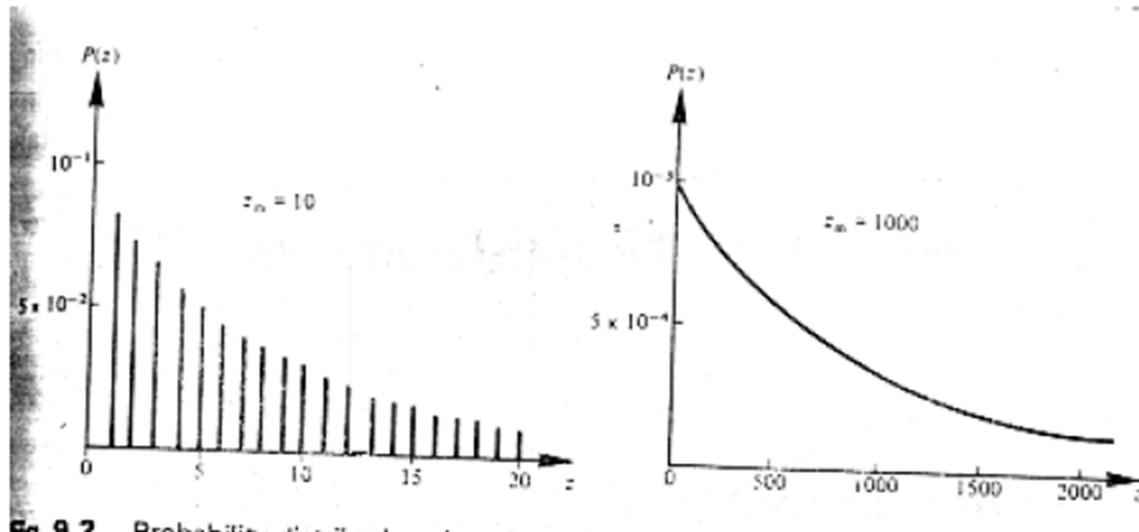


Figure 3.10.2 Probability distribution indicating the statistical fluctuations of incoherent light for $z_m = 10$ and $z_m = 1000$

The Poisson distributions for $z_m=10$ and $z_m=1000$ are illustrated in Figure 3.10.1 and represent the detection process for monochromatic coherent light. Incoherent light is emitted by independent atoms and therefore there is no phase relationship between the emitted photons. This property dictates exponential intensity distribution for incoherent light which if averaged over the Poisson distribution gives

$$P(z) = \frac{z_m^z}{(1 + z_m)^{z+1}}$$

Equation (3.10.5) is identical to the Bose Einstein distribution which is used to describe the random statistics of light emitted in black body radiation (thermal light). The statistical fluctuations for incoherent light are illustrated by the probability distributions shown in Figure

Digital signaling quantum noise:

For digital optical fiber systems it is possible to calculate a fundamental lower limit to the energy that a pulse of light must contain in order to be detected with a given probability of error. The premise on which this analysis is based is that the ideal receiver has a sufficiently low amplifier noise to detect the displacement current of a single electron hole pair generated within the detector (i.e. an individual photon may be detected). Thus in the absence of light, and neglecting dark current, no current will flow. Therefore the only way an error can occur is if a light pulse is present and no electron hole pairs are generated. The probability of no pairs being generated when a light pulse is present may be obtained from Eq. (3.10.3) and is given by:

$$P(0/1) = \exp(-z_m)$$

Thus in the receiver described $P(0/1)$ represents the system error probability $P(e)$

and therefore:

$$P(0/1) = \exp(-z_m)$$

However, it must be noted that the above analysis assumes that the photo detector emits no electron hole pairs in the absence of illumination. In this sense it is considered perfect. Equation (3.10.7) therefore represents absolute receiver sensitivity and allows the determination of a fundamental limit in digital optical communications. This is the minimum pulse energy

E_{\min} required to maintain a given bit error rate (BER) which any practical receiver must satisfy and is known as the quantum limit.

Analog transmission quantum noise:

In analog optical fiber systems quantum noise manifests itself as shot noise which also has Poisson statistics (Ref. 1]. The shot noise current is on the photocurrent I_p , is given by:

$$\overline{i_s^2} = 2eBI_p$$

Neglecting other sources of noise the SNR at the receiver may be written as:

$$\frac{S}{N} = \frac{I_p^2}{\overline{i_s^2}}$$

Substituting i_s^* is Eq. (3.10.8) gives:

$$\frac{S}{N} = \frac{I_p}{2eB}$$

The expression for the photocurrent I_p , given in Eq. (3.8) allows the SNR to be obtained in terms of the incident optical power P_o .

$$\frac{S}{N} = \frac{\eta P_o e}{h f 2eB} = \frac{\eta P_o}{2h f B}$$

Equation (3.10.1 1) allows calculation of the incident optical power required at the receiver in order to obtain a specified SNR when considering quantum noise in analog optical fiber systems.